

A&A manuscript no.

(will be inserted by hand later)

Your thesaurus codes are:

4(11.09.1: Mrk 509, MCG+8-11-11; 11.19.1; 13.25.2)

ASTRONOMY
AND
ASTROPHYSICS
26.10.2018

BeppoSAX observations of Mrk 509 and MCG +8-11-11

G. C. Perola¹, G. Matt¹, F. Fiore², P. Grandi³, M. Guainazzi⁴, F. Haardt⁵, L. Maraschi⁶, T. Mineo⁷, F. Nicastro⁸, and L. Piro³

¹ Dipartimento di Fisica, Università degli Studi “Roma Tre”, Via della Vasca Navale 84, I-00146 Roma, Italy

² Osservatorio Astronomico di Roma, Via dell'Osservatorio, I-00044 Monteporzio Catone, Italy

³ Istituto di Astrofisica Spaziale, C.N.R., Via Fosso del Cavaliere, I-00133 Roma, Italy

⁴ XMM SOC, VILSPA-ESA, Apartado 50727, E-28080 Madrid, Spain

⁵ Dipartimento di Scienze, Università dell'Insubria, Via Lucini 3, I-22100 Como, Italy

⁶ Osservatorio Astronomico di Brera, Via Brera 28, I-20121 Milano, Italy

⁷ Istituto di Fisica Cosmica ed Applicazioni all'Informatica, C.N.R., Via U. La Malfa 153, I-90146 Palermo, Italy

⁸ Harvard-Smithsonian Center for Astrophysics, 60 Garden st., Cambridge MA 02138 USA

Received February 8, 2000 / Accepted

Abstract. BeppoSAX observations of the Seyfert galaxies Mrk 509 and MCG +8-11-11 are presented. Earlier evidence of a soft excess in Mrk 509 is confirmed. This excess is found to be better represented by a power law than by a black body: with a photon slope Γ_s of 2.5, its extrapolation matches the flux recorded in the far UV. An ASCA observation, which appeared to exclude the presence of the excess while showing instead evidence of a warm absorber, turns out to be compatible with the coexistence of the excess seen with BeppoSAX and of the warm absorber. The hard power law of Mrk 509 is seen for the first time to be affected by a cut-off at high energies, with an e-folding energy of about 70 keV. In MCG +8-11-11 the cut-off is found at about 170 keV, consistent within the combined errors with a previous estimate from a ASCA+OSSE/CGRO observation. In both objects the reflection component is clearly detected. In Mrk 509 its strength, together with that of the iron K line, indicates a solid angle Ω , subtended by the reprocessing gas in the accretion disk, much less than 2π , but lacking a valid constraint on the inclination angle this evidence is not as convincing as that found with BeppoSAX in IC 4329A. In MCG +8-11-11 the same parameters are instead consistent with $\Omega=2\pi$, but the comparison with an ASCA observation, when the flux level was about 2.5 times weaker, suggests that a substantial fraction of the angle might be associated with gas farther out than the accretion disk.

Key words: Galaxies: individual: Mrk 509, MCG +8-11-11 – Galaxies: Seyfert – X-rays: galaxies

1. Introduction

As part of a broad band spectral survey, with the BeppoSAX satellite, of a sample of bright Seyfert 1 galaxies (2–10 keV flux greater than 1–2 mCrab), this paper follows those on NGC 4593 (Guainazzi et al. 1999) and IC 4329A (Perola et al. 1999), where the goals of the program are described in detail. In short terms, the survey aims at determining the parameters of the various spectral components typical of Seyfert 1s, and especially of the broad ones, with better confidence than could be done before, by exploiting the opportunity to cover simultaneously the band 0.1–200 keV, offered by the Narrow Field Instruments (NFI) onboard BeppoSAX.

This paper reports on the observations of two objects, namely Mrk 509 and MCG +8-11-11. Mrk 509 is a Seyfert 1.0 galaxy at $z=0.0344$ with a luminosity $L(2-10 \text{ keV}) \sim 3 \times 10^{44} \text{ erg s}^{-1}$ ($H_0 = 50 \text{ km s}^{-1} \text{ Mpc}^{-1}$). The galactic interstellar column toward this object amounts to $N_{H,g}=4.4 \times 10^{20} \text{ cm}^{-2}$ (Murphy et al. 1996).

MCG +8-11-11 is a Seyfert 1.5 galaxy at $z=0.0205$ with a luminosity $L(2-10 \text{ keV}) \sim 10^{44} \text{ erg s}^{-1}$. Because of the low galactic latitude ($b=10.4^\circ$) its spectrum is absorbed by a large galactic column, $N_{H,g}=2.03 \times 10^{21} \text{ cm}^{-2}$ (Elvis et al. 1989).

Special reasons of interest from earlier observations of the two objects are the following. In Mrk 509 the report of a sizeable soft excess below about 1 keV in Ginga and ROSAT simultaneous observations by Pounds et al. (1994), which appeared to confirm previous claims in data from HEAO-1 (Singh et al. 1985), EXOSAT (Morini et al. 1987) and Ginga (Singh et al. 1990), was itself not confirmed in one ASCA observation by Reynolds (1997) and by George et al. (1998), who claim instead evidence of a warm absorber. In MCG +8-11-11 a high energy cut-off

in the power law was detected in simultaneous ASCA and OSSE/CGRO observations at about 270 keV (Grandi et al. 1998).

Observations and data reduction are described in Sect. 2, the spectral analysis in Sect. 3. The results are commented and compared with previous ones in Sect. 4, and the conclusions are drawn in Sect. 5.

2. Observations and data reduction

The data used in this paper were collected from three of the four NFI on the Italian-Dutch satellite BeppoSAX (Boella et al., 1997a), namely the imaging instruments LECS (0.1–10 keV, Parmar et al. 1997) and MECS (1.8–10.5 keV, Boella et al. 1997b), and the collimated instrument PDS (13–200 keV, Frontera et al. 1997), with the collimator in the rocking mode to monitor the background. Because of remaining uncertainties in the LECS data above 4 keV, these will be ignored in the spectral analysis.

In Table 1 start dates of the observations, net exposure times and net average count rates are given. While those of MECS and PDS are comparable, the exposure times of the LECS are much shorter because this instrument is operated only during the night time fraction of the orbit. The reduction procedures and screening criteria adopted are standard (see Guainazzi et al. 1999). In particular, of the two options available for the PDS data, the Rise Time selection was used.

The spectral counts were extracted from a circular region of 4' and 8' radius around the source centroid in the MECS and LECS images respectively. The background was subtracted using spectra from blank sky files in the same position of the detectors. Due to the low galactic latitude of MCG +8-11-11, this procedure overestimates the background below about 0.4 keV: ignoring the counts below 0.4 keV, as we shall do, is of no practical consequence in the spectral fitting, due to the large value of $N_{H,g}$.

Spectra and light curves from the PDS were obtained from direct subtraction of the off- from the on-source products. The enquiry on the presence of sources that could significantly contaminate the target signal in the 1.3° FWHM field of view gave negative results.

During the observations both objects underwent intensity variations, whose detailed study goes beyond the scope of this paper. A hardness ratio analysis of the counts shows at best marginal evidence of spectral variations, hence we feel justified in applying the spectral analysis to the integrated counts. In particular the two parts of the observation of Mrk 509 will be combined. To take care of the inhomogeneity in the time coverage between LECS and MECS, we shall let their relative normalization as a free parameter. The normalization of the PDS to the MECS will instead be held fixed.

3. Spectral analysis

The analysis of the integral spectral counts, from the three instruments together, was performed with XSPEC (version 10). In the first step a “Baseline Model Spectrum” (BMS) is adopted, composed of: a Power Law with an exponential cut-off (PL), $AE^{-\Gamma} \exp(-E/E_f)$; a Reflection Component (RC), with $r = \Omega/2\pi$, the solid angle fraction of a neutral, plane parallel slab illuminated by the PL photons, and with the inclination angle i set, for reference, equal to 0° (this angle, if left free, is too loosely constrained, see Perola et al. 1999); a uniform neutral column of absorbing gas at the object redshift, N_H , in addition to the galactic $N_{H,g}$ (in both slab and column the element abundances are the cosmic values in Anders & Grevesse 1993); a gaussian iron K line, with energy E_k , width σ_k and intensity I_k (also given as an EW). Further steps include, in both objects: the addition of the OVII (0.74 keV) and OVIII (0.87 keV) edges, with their optical depths τ as free parameters, as the most direct way to verify the existence of a warm absorber (WA); the relativistic description of the iron line profile; in Mrk 509 the addition of a soft broad component.

The energy bins chosen represent about one third of the instrumental resolution, which is a function of the energy. The normalization C of the PDS relative to the MECS was adopted equal to 0.8 (Fiore et al. 1999). The “statistical” errors correspond to the 90% confidence interval for two interesting parameters, or $\Delta\chi^2=4.61$. The energy E_k is always given as in the frame of the host galaxy.

3.1. Mrk 509

Although the fit *without* the emission line gives a much worse χ^2 , in the BMS fit E_k is ill-determined, and, when E_k is fixed at 6.4 keV (or any other value up to 6.9 keV), the line width turns out to be very large, about 2.9 keV (with EW~950). The $\chi^2=176.8/137$, to be compared with 245.4/139 without the line. The addition of the two O edges leads to a substantial improvement in χ^2 , but the problem with E_k and σ_k remains. When E_k is fixed at 6.4 keV, $\chi^2=154.9/135$. The results are given in Table 2 under BMS+WA. Compared with the results obtained by Reynolds (1997), for the same model except for the absence of the RC, the optical depths are consistent, whereas his estimate of $N_H=2.1(\pm 0.6)\times 10^{20} \text{ cm}^{-2}$ is incompatible with our upper limit (the same holds with $N_{H,g}=4.2\times 10^{20} \text{ cm}^{-2}$, as adopted by Reynolds). The other parameters remain similar to those of the pure BMS fit. The extremely large value of σ_k is likely due to a bad description of the continuum at the line energy, which would affect also the determination of r . The ratio data/model when both I_k and r are set to zero (Fig. 1) indicates that the continuum becomes substantially harder above 2–3 keV, and therefore the fit manages to reproduce the data by freely

Table 1. Observation epochs and mean count rates. The count rate for the MECS refers to two units

	Start date	LECS		MECS		PDS	
		t _{exp} (s)	CR (cts s ⁻¹) (0.1-4 keV)	t _{exp} (s)	CR (cts s ⁻¹) (1.8-10.5 keV)	t _{exp} (s)	CR (cts s ⁻¹) (13-200 keV)
Mrk 509 (part 1)	1998-May-18 (12h 22m 24s UT)	23598	0.464±0.004	51864	0.601±0.003	48102	0.73±0.04
Mrk 509 (part 2)	1998-Oct-11 (04h 34m 07s UT)	18188	0.590±0.006	35970	0.736±0.005	34000	0.87±0.04
MCG +8-11-11	1998-Oct-7 (23h 10m 45s UT)	29840	0.346±0.003	74866	0.637±0.003	72472	0.98±0.04

Table 2. Spectral fits (cos $i=1$)

	Mrk 509	Mrk 509	MCG +8-11-11
	BMS + WA	BMS + SPL + WA	BMS + WA
F(2-10 keV) ^a	5.66±0.03	5.66±0.03	5.61±0.03
N _H (10 ²⁰ cm ⁻²) ^b	<0.1	0.1 ^{+0.4} _{-0.1}	<2.3
A (10 ⁻² cm ⁻² s ⁻¹ keV ⁻¹)	2.12	0.89	1.66
Γ	2.11 ^{+0.02} _{-0.03}	1.58 ^{+0.08} _{-0.09} ^d	1.84±0.05
E _f (keV)	302 ⁺¹⁵⁶⁴ ₋₁₆₂	67 ⁺³⁰ ₋₂₀ ^d	169 ⁺³¹⁸ ₋₇₈
<i>r</i>	1.99 ^{+0.51} _{-0.42}	0.57 ^{+0.34} _{-0.32} ^d	0.98 ^{+0.56} _{-0.39}
E _k (keV) ^c	6.4 (fix)	6.70 ^{+0.38} _{-0.26} ^d	6.49 ^{+0.14} _{-0.13}
σ _k (keV)	2.92 ^{+1.20} _{-0.67}	0.36 ^{+0.76} _{-0.36} ^d	0.17 ^{+0.30} _{-0.17}
I _k (10 ⁻⁴ cm ⁻² s ⁻¹)	6.1 ^{+2.2} _{-1.8}	0.62 ^{+0.76} _{-0.35} ^d	0.81 ^{+0.45} _{-0.33}
EW (eV)	980 ⁺³⁵³ ₋₂₈₉	107 ⁺¹³⁰ ₋₆₀ ^d	133 ⁺⁷⁴ ₋₅₄
τ(O VII)	0.15 ^{+0.14} _{-0.13}	0.06 ^{+0.11} _{-0.06} ^d	0.17 ^{+0.19} _{-0.17}
τ(O VIII)	<0.17	<0.08 ^d	<0.18
A _s (10 ⁻² cm ⁻² s ⁻¹ keV ⁻¹)	–	1.11	–
Γ _s	–	2.50 ^{+0.94} _{-0.25} ^e	–
χ ² /d.o.f.	154.9/135	134.5/132	113.7/130

^aAs observed in 10⁻¹¹ erg cm⁻² s⁻¹.^bIn excess of N_{H,g}=4.4×10²⁰ cm⁻² (Mrk 509), 2.03×10²¹ cm⁻² (MCG +8-11-11).^cIn the frame of the host galaxy.^dErrors computed with N_H and Γ_s frozen at their best fit values.^eErrors computed with N_H frozen at its best fit value.

adjusting I_k , σ_k and r . On the other hand in the same plot the presence of a (much narrower) iron emission line is evident. For completeness, we report that the use of the module ABSORI in XSPEC, as a more detailed description of the warm absorber than the two edges, leads to the same value of Γ (2.11), hence to the same problem with σ_k and r .

To further investigate this aspect, we fitted the LECS data with a simple power law absorbed by N_H. The χ^2

is 142/53, and the ratio data/model in Fig. 2 shows a curvature in the slope. The curvature remains after the addition of the two edges, which brings the χ^2 down to 115/51, a still fully unacceptable value. Some improvement is achieved using ABSORI, but the $\chi^2 = 89/51$ remains unacceptable.

We therefore decided to describe this situation by adding to the BMS another broad component, referred to as a Soft Power Law (SPL: $A \cdot E^{-\Gamma_s}$). The line on

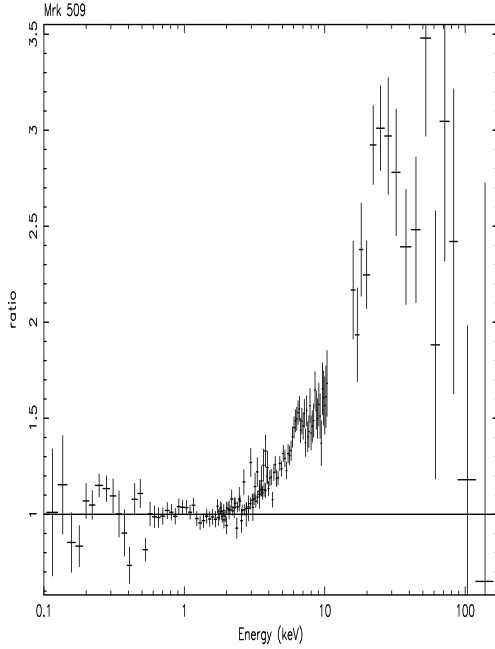


Fig. 1. Mrk 509. Ratio of LECS, MECS and PDS data to the model BMS+WA, when the parameter values are those given in Table 2, except for I_k and r , which are set equal to zero.

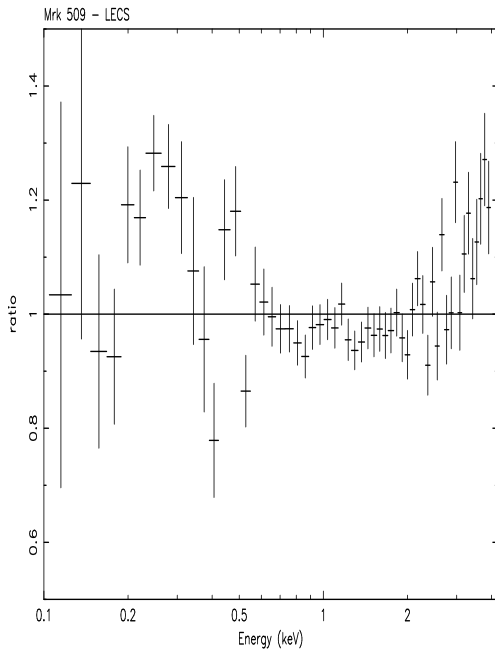


Fig. 2. Mrk 509. Ratio data to model, when the LECS data are fitted with a simple power law, absorbed by $N_{H,g}$.

ergy is now reasonably well determined, hence this fit includes three more free parameters relative to the BMS. The $\chi^2=135.6/134$, and the outcome is dramatically different: along with a much harder slope Γ and a much smaller reflection r , σ_k is about 0.4 keV only (EW \sim 100 eV); moreover, E_f shifts from about 300 to about 70 keV. The addition of the two edges leads now to no significant improvement ($\chi^2=134.5/132$) and only OVII is at best marginally detected. The high significance of the line and of the cut-off is instead demonstrated by comparing the χ^2 given above with those obtained without the line, 154.5/135, and without both line and cut-off, 212.9/136.

The results, under BMS+SPL+WA, are given in Table 2 and illustrated in Fig. 3. Note that again N_H is negligible compared to $N_{H,g}$. To avoid their strong interplay with Γ , both N_H and Γ_s were frozen at their best fit values when the errors on all the other parameters, given in Table 2, were determined; likewise the confidence contours for the couples (Γ, r) , (Γ, E_f) , and (E_k, σ_k) , given in Fig. 4, 5 and 6, were also obtained. Caution is therefore due when discussing single parameters, in particular the marginal evidence that the value of E_k in Table 2 is larger than the neutral value of 6.4 keV should be regarded as hardly significant. As an independent test, we checked whether a partially ionized reflector was preferable, and obtained a best fit value of zero for the ionization parameter.

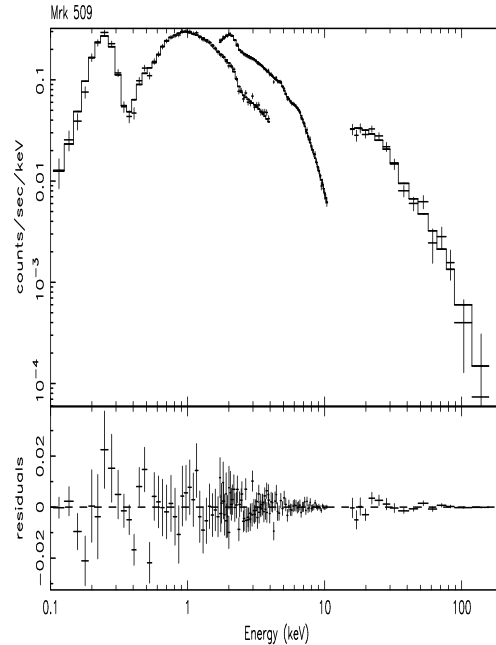


Fig. 3. Mrk 509. LECS, MECS and PDS spectra with the best fit BMS+SPL+WA given in Table 2 (upper panel), and residuals (lower panel).

Since the iron line is marginally resolved, we tried the relativistic profile description for an accretion disk around

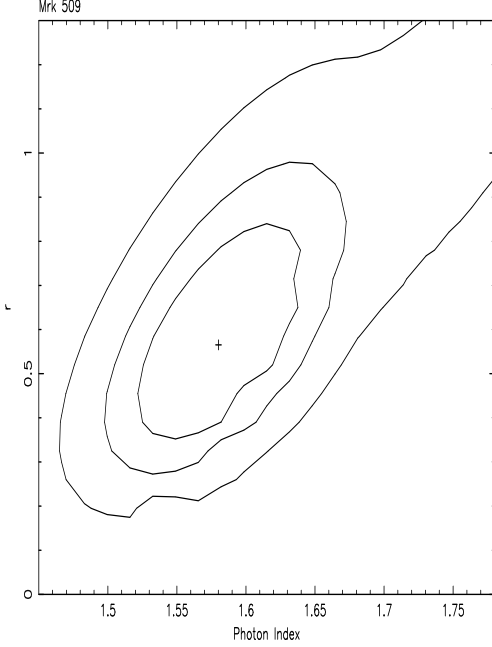


Fig. 4. Mrk 509. Confidence (67, 90, 99%) contours of Γ and r in the BMS+SPL+WA fit given in Table 2, obtained with N_H and Γ_s frozen at their best fit values.

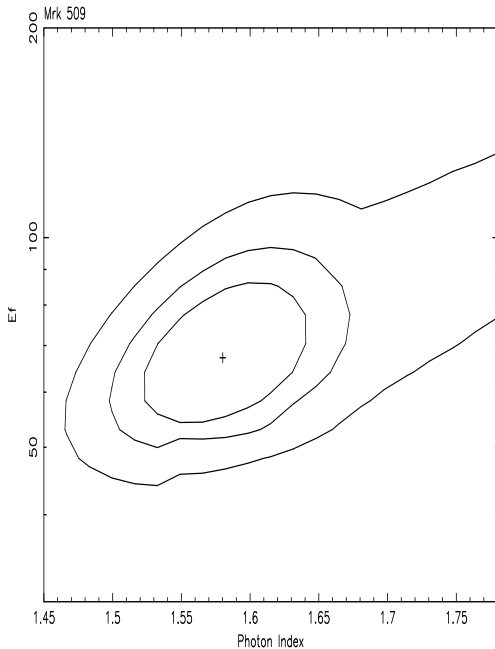


Fig. 5. Mrk 509. Confidence (67, 90, 99%) contours of Γ and E_f in the BMS+SPL+WA fit given in Table 2, obtained with N_H and Γ_s frozen at their best fit values.

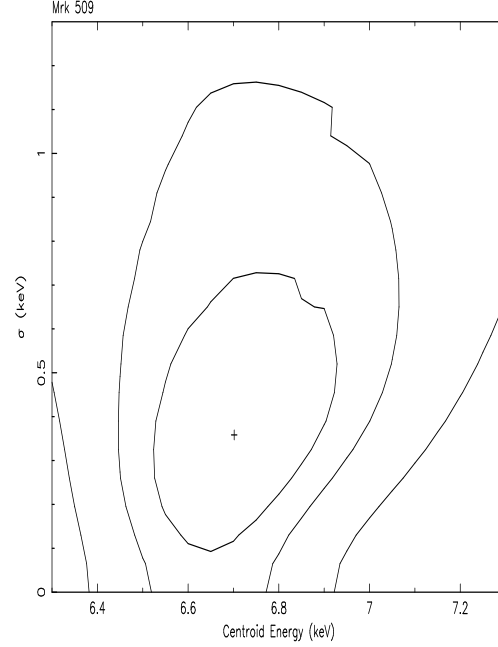


Fig. 6. Mrk 509. Confidence (67, 90, 99%) contours of E_k and σ_k in the BMS+SPL+WA fit given in Table 2, obtained with N_H and Γ_s frozen at their best fit values.

a Schwarzschild black hole, with the inner radius $R_i=6 r_g$ and the emissivity slope $\beta=-2$ fixed: the line energy, the outer radius R_{out} , the intensity and the inclination angle being the free parameters. The angle in the RC component was linked to that of the disk, the main goal of this exercise being to provide a constraint on i . The χ^2 is comparable to that of the gaussian description. The inclination angle is 56° , but at the 90% confidence level it could be anything between 0° and 87° ; this reflects itself into a 90% interval for r ranging from 0.35 to 3.8. In practice no useful constraint is obtained on i , $R_{out} \sim 2900$, and all other parameter values remain very similar to those in Table 2.

The comparison between the two parts of the observation, fitted independently, shows no significant differences in the spectral parameters. In particular for the parameters of the broad components in the first (second) part of the observation we obtain: $\Gamma_s = 2.46^{+2.02}_{-0.33}$ ($\Gamma_s = 2.72^{+1.92}_{-0.40}$), $\Gamma = 1.64^{+0.11}_{-0.17}$ ($\Gamma = 1.74^{+0.22}_{-0.11}$), $E_f = 79^{+60}_{-29}$ keV ($E_f = 80^{+158}_{-30}$ keV), $r = 0.64^{+0.56}_{-0.44}$ ($r = 0.83^{+0.76}_{-0.47}$). A joint fit of the two parts, with all parameters linked (that is the same) except for the normalizations, gives a very good $\chi^2 = 285/277$: the ratios of the soft and of the hard PL intensities between the first and the second part are equal to 1:1.40 and 1:1.21 respectively, thus indicating that both components increased, but the SPL more than the hard PL.

As an alternative to the SPL, we tested the black body description of the soft excess, which was adopted by Pounds et al. (1994). The $\chi^2 = 137.6/132$ is perfectly acceptable, and $kT_s = 0.07$ keV, but, although somewhat

smaller than those from the BMS+WA fit, the values $\sigma_k = 2.3$ keV and $EW = 580$ eV remain improbably large, and lead us to believe that the SPL option is to be preferred.

3.2. MCG +8-11-11

The BMS fit (above 0.4 keV) yields $\chi^2=117.5/132$. The addition of the two edges leads to a slight decrease, $\chi^2=113.7/130$, and only OVII is marginally detected. The results of this fit are given in Table 2 under BMS+WA and shown in Fig. 7. They are further illustrated as confidence contours for the couples (Γ, r) , (Γ, E_f) , and (E_k, σ_k) in Fig. 8, 9, 10. The significance of the line and of the cut-off is further demonstrated by the χ^2 obtained without the line (155/133) and without both line and cut-off (189.6/134). The iron line, consistent in energy with 6.4 keV, is not resolved. The fit with a relativistic profile gives essentially the same EW, and no useful information on the inclination angle. Albeit marginal, the detection of a warm absorber is new in this object. Note, on the other hand, that the intrinsic, cold N_H is negligible compared to $N_{H,g}$.

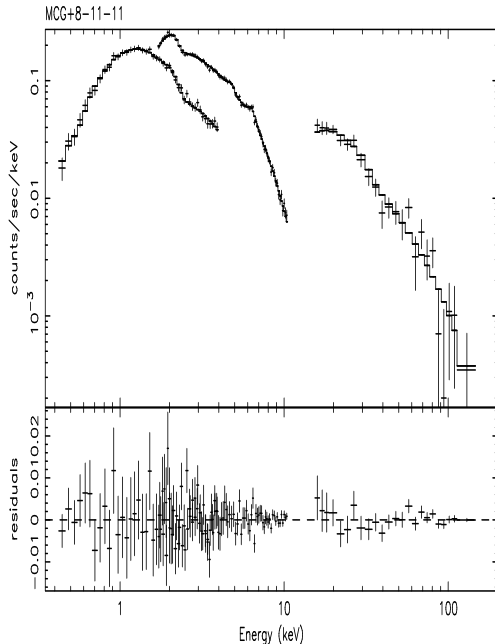


Fig. 7. MCG +8-11-11. LECS, MECS and PDS spectra with the best fit BMS+WA given in Table 2 (upper panel), and residuals (lower panel).

4. Comments and comparison with previous results

4.1. Mrk 509

We believe that the BeppoSAX data, thanks to their major asset, namely the very broad band, demonstrate that

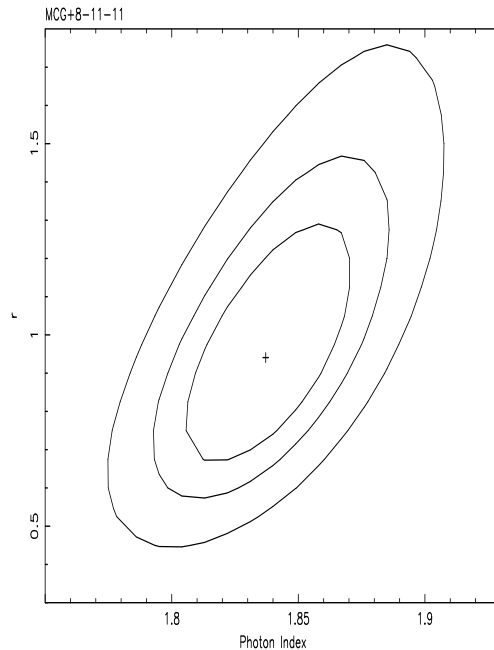


Fig. 8. MCG +8-11-11. Confidence (67, 90, 99%) contours of Γ and r in the BMS+WA fit given in Table 2.

the continuum is steeper at low than at high energies ($\Delta\Gamma \sim 0.9$), thus confirming that reports, from measurements prior to ASCA, of a “soft excess” below about 1 keV were substantially correct. It would be important to establish whether the curvature is due to the superposition of two components (as modelled by us) or is an intrinsic property of the same physical component. The comparison between the two parts of our observation described in Sect. 3 suggests at least a physical connection between the two components. The extrapolation of the SPL to UV wavelengths is also of interest. The reddening corrected ($E(B - V)=0.08$) νf_ν at 1350 Å is given in Wang et al. (1998) to be $16.2(\pm 1.5) \times 10^{-11}$ erg cm $^{-2}$ s $^{-1}$. The extrapolation of the SPL, with A_s and Γ_s the best fit values in Table 2, gives 18.6×10^{-11} erg cm $^{-2}$ s $^{-1}$. While the near coincidence is probably fortuitous, in view of variability and the uncertainty on Γ_s , it suggests a close connection between the UV and the soft X-ray excess emission. This result is in agreement with the finding by Wang et al. (1998) in a heterogeneous sample of objects (see also Laor et al. 1997), but it adds value to it for this particular galaxy, because it is obtained extrapolating the soft excess, rather than the simple power law fitted to the ROSAT data. For an approach similar to ours, based on simultaneous ROSAT and Ginga observations of other objects, see Walter et al. (1994). Since Mrk 509 for its luminosity could be ranked among quasars, it is appropriate to note that Γ_s is close to the mean value of 2.8 in the range 350–1050 Å found by Zheng et al. (1997) in the composite HST spectrum of 41 radio-quiet quasars.

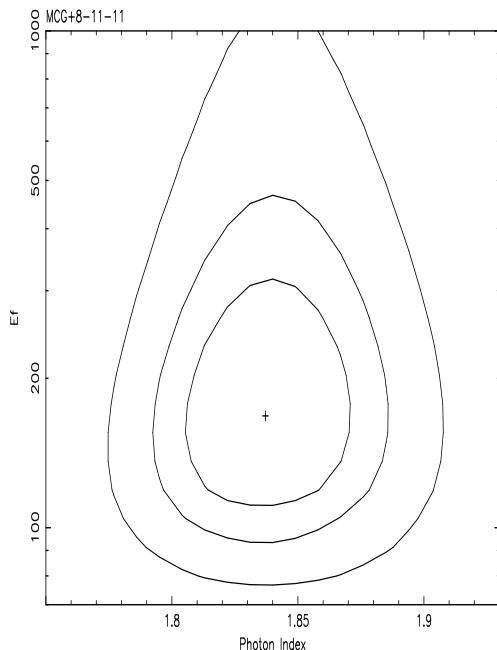


Fig. 9. MCG +8-11-11. Confidence (67, 90, 99%) contours of Γ and E_f in the BMS+WA fit given in Table 2.

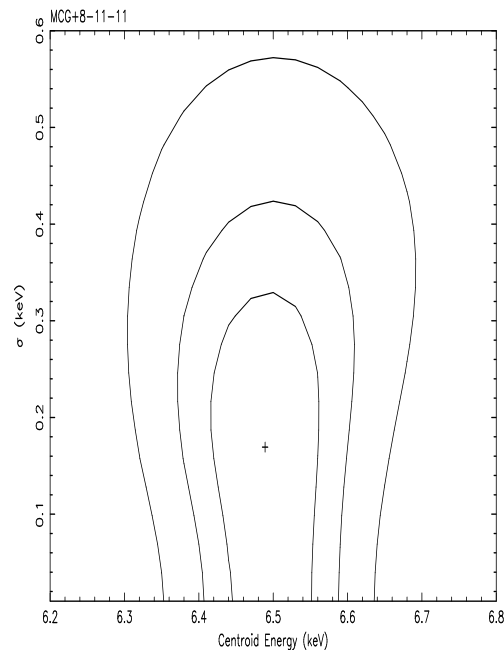


Fig. 10. MCG +8-11-11. Confidence (67, 90, 99%) contours of E_k and σ_k in the BMS+WA fit given in Table 2.

Another important property of the continuum, seen for the first time in this object, is the evidence of a cut-off occurring at $E_f \sim 70$ keV. The few other objects in which this property has been determined have best fit values greater than 100 keV (Matt 2000, and references therein), the only exception being NGC 4151 (Jourdain et al. 1992, Zdziarsky et al. 1996, Piro et al. 1998). Since Mrk 509 shares with NGC 4151 a slope much harder than the average, although not quite as hard, this results adds some confidence to the hint of a correlation between E_f and Γ found by Piro (1999).

To assess the issue of the warm absorber, we retrieved from [HTTP://TARTARUS.GSFC.NASA.GOV/](http://TARTARUS.GSFC.NASA.GOV/) the 0.6-10 keV data of the ASCA observation (1994, April 29) investigated by Reynolds (1997) and by George et al. (1998). The average intensity in the two observations is the same within 10%. As a simple compatibility test, we estimated the χ^2 when the BMS+SPL+WA model is adopted, with all parameters equal to the best fit values in Table 2, except for the normalizations A_s , A and I_k , which are left free, and with the O optical depths first set to zero. We obtain an unacceptable $\chi^2=2020/1881$. The residuals undoubtedly show the signature of the O VII edge, and upon letting the O edges also free, we obtain indeed a pretty acceptable $\chi^2=1933/1879$, with $\tau(\text{O VII}) = 0.20 \pm 0.04$ (90% for one i. p., $\Delta\chi^2=2.71$), $\tau(\text{O VIII})$ consistent with zero, a ratio $A_s/A=1.1$, within 15% of the BeppoSAX fit, and an iron line EW ~ 110 eV, similar to the BeppoSAX fit.

From this exercise we would conclude that the two independent data sets are consistent with a model which includes both a “soft excess” in the form of a steepening

of the power law below about 1 keV, as well as a warm absorber. Due to the much higher statistics and better resolution at the appropriate energies, it is not surprising that the ASCA data put a stronger and more reliable constraint on the warm absorber than our data. The $\tau(\text{O VII})$ given above is larger than $0.11^{+0.03}_{-0.04}$, the value obtained by Reynolds (1997) jointly with $N_H = 2.1 \times 10^{20} \text{ cm}^{-2}$. In our exercise an almost identical value, $\tau(\text{O VII}) = 0.10$, is obtained instead when we leave N_H free: the χ^2 drops to 1850/1878, and $N_H=3.6 \times 10^{20} \text{ cm}^{-2}$, but this column is by at least one order of magnitude incompatible with our data (see Table 2). This discrepancy, already noted in the BMS+WA fit (Sect. 3.1), is probably connected with the epoch-dependence in the response of the ASCA-SIS instruments below 1 keV, which is not yet well understood (T. Yaqoob, private communication).

For a slab seen face-on ($i=0^\circ$), the iron line EW ~ 100 eV is roughly consistent with both a normal abundance and the solid angle $\Omega \sim \pi$ corresponding to the best fit value of r (Matt et al. 1991, Matt et al. 1997). However, lacking a constraint on the inclination angle, and taking into account the uncertainties, the issue whether Ω is indeed much less than 2π , as it was rather convincingly found to be the case for the reprocessing in the accretion disk of IC 4329A (Perola et al. 1999), remains open.

4.2. MCG 8-11-11

Our estimate of r for a face-on reprocessing slab is fully consistent with an $\Omega = 2\pi$ geometry. The corresponding line EW, for iron with solar abundance, should be about

190 eV (Matt et al. 1997), larger than the best fit value of 130 eV, but marginally within the errors. The line width is too poorly constrained for us to elaborate on the contribution by the accretion disk, and note that also in the ASCA observation (Grandi et al. 1998) the line is barely resolved. We cannot exclude that a sizeable fraction of the reprocessing gas might be located further out. In this respect, comparison with the results obtained from the ASCA+OSSE observation by Grandi et al. (1998) is suggestive, since at that epoch the source was a factor 2.4 fainter. They find $\Gamma = 1.73 \pm 0.06$, $r = 1.64^{+0.88}_{-0.78}$, $EW = 230^{+222}_{-99}$ eV (errors for $\Delta\chi^2=2.71$). None of these estimates differ from ours more than the combined errors. Yet the smaller value of Γ agrees with an earlier finding (Treves et al. 1990) of a correlation between Γ and flux, while the larger values of both r and EW could be due to a lag in the response from a reprocessing material located far away from the variable PL source. More sensitive and better resolution observations might confirm this suggestion, which indicates an $\Omega \ll 2\pi$ geometry for the reprocessing in the accretion disk also in this object.

Concerning the absorption, we find for the first time an admittedly modest evidence of a warm absorber; at the same time we do not confirm the claim by Grandi et al. (1998) of a column significantly in excess of $N_{H,g}$, a discrepancy comparable to that found in Mrk 509 and likely due to the same cause.

We confirm the presence of the cut-off in the PL, with E_f about 170 keV, smaller than the value 266^{+90}_{-68} keV found by Grandi et al. (1998), but consistent within the combined errors.

5. Conclusions

A particularly interesting result of the present study is the overall shape of the "direct" continuum in Mrk 509, which can be empirically described as a combination of two power laws. The soft power law we detect is, in the first place, a confirmation of earlier evidence of a low energy excess (see Sect. 1), and it seems to us a better description of the excess than the simple black body adopted by Pounds et al. (1994). With a slope Γ_s about 2.5, it appears as a continuation into the X-rays of the UV emission, and according to models sometimes invoked for this component (e. g. by Zheng et al. 1997, but see also Walter et al. 1994, Fiore et al. 1995, Laor et al. 1997 for a broader discussion of the problem), it could arise from comptonization in the innermost parts of the disk in regimes of high accretion rate (e. g. Czerny & Elvis 1987, Maraschi & Molendi 1990). The hard power law is affected by a high energy cut-off, which can be empirically described as an exponential factor with E_f about 70 keV. The currently most popular models for this component involve comptonization by a hot corona (e. g. Haardt & Maraschi 1993, Zdziarsky et al. 1994, Ghisellini et al. 1998), in which the cut-off is related to the temperature of the corona. Our results on Mrk

509 are similar to those on NGC 4151, possibly indicating that Seyferts with unusually flat continua feature unusually low cut-off energies (Piro 1999). However it is fair to say that proper, selfconsistent models need to be used in the fits in order to recover correctly the physical parameters. As extensively discussed by Petrucci et al. (2000) in the context of a BeppoSAX observation of NGC 5548, the exponential cut-off powerlaw is indeed a quite rough approximation to realistic comptonization models.

Overall the spectrum of Mrk 509 requires a complex structure for the accretion disk, to explain both the soft and the hard components. This will be dealt with in a future paper, where we would like to address the problem in a comprehensive manner for all the objects in the BeppoSAX sample of bright Seyfert 1. There we shall include also a more advanced analysis of the comptonization model, underlying the continuum shape and in particular the high energy cut-off seen in MCG +8-11-11, already discussed in Grandi et al. (1998).

This approach will also attempt to deal selfconsistently with the "reprocessed" spectral components, namely the amount of continuum reflection along with the energy/width/intensity of the iron line, contributed by the matter in the accretion disk. Here we limit ourselves to note that, although not conclusively yet, directly from this observation in Mrk 509 and from comparison with an ASCA observation in MCG +8-11-11, there are indications of the accretion disk contributing to the reprocessing much less than one would expect if the solid angle Ω were 2π . Such a situation was also, and rather more convincingly found to hold in IC 4329A (Perola et al. 1999).

Finally, in both Mrk 509 and MCG +8-11-11 our observations present some evidence of a warm absorber. This evidence is roughly consistent with the more significant one found with ASCA in Mrk 509 by Reynolds (1997) and by George et al. (1998), who did not however confirm in their analysis the presence of a soft excess. We have shown that the ASCA data are compatible with the coexistence of the warm absorber together with the soft excess observed by BeppoSAX. While doing that, we have noted that the interpretation of the ASCA data is complicated by a not yet perfectly understood, epoch-dependent, problem with the response in the ASCA-SIS low energy channels (T. Yaqoob, private communication): the implication (which is noted to be present, but with less of a consequence, in the ASCA observation of MCG +8-11-11, Grandi et al. 1998) is equivalent to an additional N_H of a few 10^{20} cm^{-2} , which is largely incompatible with our data.

Acknowledgements. The BeppoSAX satellite is a joint Italian-Dutch program. We wish to thank the Scientific Data Centre for assistance. This research has made use of the TARABUS database, which is supported by Jan. Turner and Kim.

pal Nandra under NASA grants NAG5-7385 and NAG5-7067, and of the NASA/IPAC Extragalactic Database (NED) which is operated by the Jet Propulsion Laboratory, California Institute of Technology, under contract with the National Aeronautics and Space Administration. This work was supported by the Italian Space Agency, and by the Ministry for University and Research (MURST) under grant COFIN98-02-32.

References

- Anders E., Grevesse N., 1993, *Geochim. Cosmochim. Acta* 53, 197
- Boella G., Butler R. C., Perola G. C., et al., 1997a, *A&AS* 122, 299
- Boella G., Chiappetti L., Conti G., et al., 1997b, *A&AS* 122, 327
- Czerny B., Elvis M., 1987, *ApJ* 321, 305
- Elvis M., Lockman F. J., Wilkes B., 1989, *AJ* 97, 777
- Fiore F., Elvis M., Siemiginowska A., et al., 1995, *ApJ* 449, 74
- Fiore F., Guainazzi M., Grandi P., 1999, SDC report (ftp://www.sdc.asi.it/pub/sax/doc/software_docs/saxabc.v1.2.ps.gz)
- Frontera F., Costa E., Dal Fiume D., et al., 1997, *A&AS* 122, 357
- George I. M., Turner T. J., Netzer H., et al., 1998, *ApJS* 114, 73
- Ghisellini G., Haardt F., Svensson R., 1998, *MNRAS* 297, 348
- Grandi P., Haardt F., Ghisellini G., et al., 1998, *ApJ* 498, 220
- Guainazzi M., Perola G. C., Matt G., et al., 1999, *A&A* 346, 407
- Haardt F., Maraschi L., 1993, *ApJ* 413, 507
- Jourdain E., Bassani L., Buchet L., et al., 1992, *A&A* 256, L38
- Laor A., Fiore F., Elvis M., Wilkes B. J., McDowell J. C., 1997, *ApJ* 477, 93
- Maraschi L., Molendi S., 1990, *ApJ* 353, 452
- Matt G., 2000, *Astron. Lett. & Comm.*, submitted
- Matt G., Perola G. C., Piro L., 1991, *A&A* 247, 25
- Matt G., Fabian A. C., Reynolds C. S., 1997, *MNRAS* 289, 175
- Morini M., Lipani N. A., Molteni D., 1987, *ApJ* 317, 145
- Murphy E. M., Lockman F. J., Laor A., Elvis M., 1996, *ApJS* 105, 369
- Parmar A. N., Martin D. D. E., Bavdaz M., et al., 1997, *A&AS* 122, 309
- Perola G. C., Matt G., Cappi M., et al., 1999, *A&A* 351, 937
- Petrucchi P. O., Haardt F., Maraschi L., et al., 2000, *ApJ*, submitted
- Piro L., 1999, *Astron. Nachr.* 320, 236
- Piro L., Nicastro F., Feroci M., et al., 1998, *Nucl. Phys. B (Proc. Suppl.)* 69, 481
- Pounds K. A., Nandra K., Fink H. H., Makino F., 1994, *MNRAS* 267, 193
- Reynolds C. S., 1997, *MNRAS* 286, 513
- Singh K. P., Garmire G. P., Nousek J., 1985, *ApJ* 297, 633
- Singh K. P., Westergaard N. J., Schnopper H. W., Awaki H., Tawara Y., 1990, *ApJ* 363, 131
- Treves A., Bonelli G., Chiappetti L., et al., 1990, *ApJ* 359, 98
- Walter R., Orr A., Courvoisier T. J.-L., et al., 1994, *A&A* 285, 119
- Wang T. G., Lü Y. J., Zhou Y. Y., 1998, *ApJ* 493, 1
- Zdziarski A. A., Fabian A. C., Nandra K., et al., 1994, *MNRAS* 269, L55
- Zdziarski A. A., Johnson W. N., Magdziarz P., 1996, *MNRAS* 283, 193
- Zheng W., Kriss G. A., Telfer R. C., Grimes J. P., Davidsen A. F., 1997, *ApJ* 475, 469